

hMOF Acetylation of DBC1/CCAR2 Prevents Binding and Inhibition of SirT1

Hong Zheng, Leixiang Yang, Lirong Peng, Victoria Izumi, John Koomen, Edward Seto, Jiandong Chen

Molecular Oncology Department, Moffitt Cancer Center, Tampa, Florida, USA

The NAD⁺-dependent deacetylase SirT1 regulates gene silencing and genomic stability in response to nutrient deprivation and DNA damage. An important regulator of SirT1 in mammalian cells is DBC1 (deleted in breast cancer 1; KIAA1967 or CCAR2), which binds to SirT1 and inhibits the deacetylation of substrates. Recent studies have revealed that ATM/ATR-mediated phosphorylation of DBC1 promotes binding to SirT1. Here we show that DBC1 is modified by acetylation on two N-terminal lysine residues (K112 and K215). The MYST family histone acetyltransferase hMOF (human MOF) is responsible for DBC1 acetylation. Acetylation of K112 and K215 inhibits DBC1-SirT1 binding and increases SirT1 deacetylase activity. SirT1 also promotes DBC1 deacetylation, suggesting the presence of a negative-feedback mechanism that stabilizes the SirT1-DBC1 complex and limits SirT1 activity. hMOF binding and acetylation of DBC1 are inhibited after DNA damage in an ATM-dependent fashion, contributing to increased SirT1-DBC1 binding after DNA damage. Furthermore, a DBC1 mutant that mimics the acetylated state fails to promote apoptosis after DNA damage. These results suggest that acetylation of DBC1 inhibits binding to SirT1 and serves as a mechanism that connects DNA damage signaling to SirT1 and cell fate determination.

The silent information regulator 2 (Sir2) is a NAD⁺-dependent deacetylase that regulates chromatin silencing in *Saccharomyces cerevisiae* (1). The mammalian homolog of Sir2 (SirT1) regulates glucose homeostasis, DNA repair, and rRNA transcription (2–6). SirT1 deficiency also predisposes mice to genomic instability and tumors in the p53 heterozygous background (7). SirT1 functions through regulation of histone acetylation and heterochromatin formation (1). When targeted to promoters by other proteins, SirT1 deacetylates histones H4 K16 and H3 K9, and recruits histone H1 to promote the establishment of repressed chromatin (8). SirT1 also deacetylates many nonhistone proteins such as p53, Foxo, and Ku70 to regulate sensitivity to apoptosis (3, 9–12).

Sir2 in yeast functions as part of the SIR complex (13). Similarly, mammalian SirT1 interacts with other chromatin-modifying enzymes to form multimeric complexes in which different enzymes act in a sequential or coordinated fashion. An interesting example is the interaction between SirT1 and SUV39H1 (5, 14). SirT1 interacts with the N-terminal chromo domain of SUV39H1 and deacetylates SUV39H1 on K266 to stimulate its histone methyltransferase activity. SirT1 and SUV39H1 also interact with the nucleolar protein nucleomethylin (NML) to repress rRNA transcription (5). The activity and function of SirT1 are regulated at multiple levels. Recruitment into specific complexes, such as the nucleolar repression complex eNoSC, by NML is important for the regulation of rRNA transcription (5). SirT1 activity is also regulated by NAD⁺ level (15), phosphorylation (16), and interaction with the activator protein AROS (17).

Recent studies revealed that SirT1 interacts with and is inhibited by the protein DBC1 (deleted in breast cancer 1; KIAA1967 or CCAR2) (18, 19). DBC1 is a nuclear protein of 923 residues with partial sequence homology to CCAR1/CARP1. It was recently redesignated CCAR2 (cell cycle activator and apoptosis regulator 2) to distinguish it from an unrelated protein with an identical name (“deleted in bladder cancer 1”) (20). DBC1 uses an N-terminal putative leucine zipper to bind to the SirT1 catalytic domain and inhibit its deacetylase activity (18). DBC1 knockdown increases

SirT1 activity and protects cells from DNA damage-induced apoptosis. The role of DBC1 as a physiological regulator of SirT1 was demonstrated by the increase in SirT1 activity in DBC1-null mice (21). *DBC1* was initially identified by its localization to a region of chromosome 8p21 that was homozygously deleted in human breast cancer (22). However, *DBC1* was not considered to be the primary target of the deletion, and its role in cancer development remains to be determined. In addition to binding SirT1, DBC1 also binds and inhibits SUV39H1 and histone deacetylase 3 (HDAC3) (23, 24). SirT1-DBC1 binding is stimulated by ATM-mediated phosphorylation of DBC1 on T454, which creates a second binding site for SirT1 that stabilizes the complex (25, 26). The regulation of SirT1-DBC1 by phosphorylation is important for cell fate determination after DNA damage.

Results described in this article suggest that SirT1-DBC1 interaction is also regulated by human MOF (hMOF)-mediated acetylation of DBC1. hMOF is a member of the MYST family of histone acetyltransferases (hMOF/MYST1, HBO1/MYST2, MOZ/MYST3, MORF/MYST4, and Tip60) (27). Members of the MYST family are involved in diverse nuclear functions, including transcription, replication, and DNA repair (28). hMOF is the human ortholog of the *Drosophila* MOF protein, which as a component of the dosage compensation complex localizes to numerous sites on the male X chromosome and equalizes X-linked gene expression between male and female flies that contain different X chromosome copies (29). Both human MOF and *Drosophila* MOF have the same acetyltransferase activity that is specific for histone H4 K16. hMOF is the major enzyme responsible for H4 K16 acetyla-

Received 8 July 2013 Returned for modification 7 September 2013

Accepted 10 October 2013

Published ahead of print 14 October 2013

Address correspondence to Jiandong Chen, Jiandong.chen@moffitt.org.

Copyright © 2013, American Society for Microbiology. All Rights Reserved.

doi:10.1128/MCB.00874-13

tion in human cells (30). Mouse MOF (mMOF) is required for viability during embryonic development (31, 32). Primary human tumors and tumor cell lines often have elevated expression of hMOF (31). hMOF has been shown to interact with ATM, facilitates ATM activation, and promotes H4 K16 acetylation after DNA damage, which may facilitate DNA repair (33). In addition to modification of histone, hMOF (and its homolog Tip60) also participates in the acetylation of p53 on K120, which enhances the ability of p53 to induce apoptosis target genes but not cell cycle targets after DNA damage (34, 35). Therefore, hMOF acetylation of nonhistone proteins may contribute to its regulatory effects on the DNA damage response and repair pathways. Interestingly, hMOF activity and stability are regulated by SirT1-mediated deacetylation (36).

In this study, we present evidence that DBC1 is modified by acetylation on two N-terminal lysine residues (K112 and K215) by hMOF. Acetylation inhibits DBC1-SirT1 binding and increases SirT1 activity. Acetylation of DBC1 is reduced after DNA damage in an ATM-dependent fashion. DBC1 mutant that mimics constitutive acetylation failed to promote apoptosis after DNA damage. The results suggest that during homeostasis, acetylation of DBC1 limits its ability to bind and inhibit SirT1. DNA damage suppresses DBC1 acetylation, stimulates DBC1-SirT1 binding, and lowers the threshold for apoptosis. Therefore, DBC1 acetylation is a novel mechanism for regulation of SirT1 activity and cell fate in response to DNA damage.

MATERIALS AND METHODS

Cell lines and reagents. H1299 (non-small cell lung carcinoma, p53 null), U2OS (osteosarcoma, p53 wild type), and A549 (lung adenocarcinoma, p53 wild type) cells were maintained in Dulbecco's modified Eagle's medium (DMEM) with 10% fetal bovine serum. Transfections of H1299 and U2OS cells were performed using the standard calcium phosphate precipitation protocol. EX-527 and etoposide were purchased from Sigma. Retrovirus expressing FLAG-DBC1 was kindly provided by Zhenkun Lou. The ATM-specific inhibitor KU-55933 was purchased from Tocris Bioscience.

IP and Western blot analysis. For immunoprecipitation (IP), cells were lysed in a buffer containing 50 mM Tris-HCl (pH 8.0), 150 mM NaCl, 5 mM EDTA, 0.5% NP-40, 1 mM phenylmethylsulfonyl fluoride (PMSF), and protease inhibitor cocktail. Lysates were incubated with primary antibodies overnight at 4°C. Immunoprecipitates were washed three times with the same buffer and fractionated by SDS-PAGE. For Western blotting (immunoblotting [IB]), proteins were transferred onto membranes, which were then incubated with the antibodies indicated in the figures. Proteins of interest were visualized using Supersignal reagent (Thermo Scientific). SirT1 was detected using 10E4 antibody (37). FLAG tag antibody was from Sigma-Aldrich. Antiactin and -hemagglutinin (HA) tag antibodies were purchased from Santa Cruz Biotechnology. DO-1 for p53 was from Pharmingen. hMOF and DBC1 antibodies were from Bethyl. AcK-p53 (K382), Ac-Lys, and Myc antibodies were from Cell Signaling.

MS analysis. Myc-tagged DBC1 was transiently transfected into H1299 cells and purified by immunoprecipitation using Myc antibody. After SDS-PAGE separation, the band containing DBC1 was excised. The protein was reduced with Tris-carboxyethylphosphine, alkylated with iodoacetamide, and digested overnight with sequencing-grade trypsin (Promega, Madison, WI). Peptides were extracted for analysis by nano-liquid chromatography-tandem mass spectrometry (nano-LC-MS/MS) (U3000 [Dionex] and LTQ-Orbitrap [Thermo, San Jose, CA]). Tandem mass spectra were matched to peptide sequences using Sequest (Thermo, San Jose, CA) and Mascot (Matrix Science, Boston, MA). Variable modifications considered in the database searches were methionine oxidation,

lysine acetylation, lysine methylation, and arginine methylation. All modified peptides were manually verified by inspection of the data.

In vitro acetylation assay. The *in vitro* acetylation assay was performed as described previously (36). Recombinant glutathione S-transferase (GST)-DBC1-1-240 (positions 1 to 240) and 1-240-dR (where dR represents double arginine substitution for K112 and K211) were incubated with or without FLAG-purified hMOF in the presence of 5 mM acetyl coenzyme A (acetyl-CoA) in reaction buffer containing 50 mM HEPES (pH 8.0), 10% glycerol, 1 mM dithiothreitol (DTT), 1 mM PMSF, and 10 mM sodium butyrate. Reaction mixtures were incubated at 30°C for 1 h, resolved on SDS-PAGE, and analyzed by immunoblotting. Protein levels were detected by Coomassie blue staining.

In vitro SirT1 deacetylation assay. SirT1 activity *in vitro* was determined with a SirT1 fluorometric kit (Biomol International) according to the manufacturer's instructions. This assay uses a lysine-acetylated peptide corresponding to K382 of human p53 as a substrate. Cultured cells were transfected with the indicated constructs. After 2 days, cells were untreated or treated with EX-527 (2 μ M) and lysed in lysis buffer as described above. Equal amounts of lysate were incubated with 50 μ M Fluor de Lys-SirT1 substrate and 500 μ M NAD⁺ in 50 μ l of reaction buffer (BML-K1286; Biomol International). The mixture was incubated for 1 h at 37°C, and the reaction was terminated by adding a solution containing Fluor de Lys developer (Enzo Life Sciences) and 2 mM nicotinamide. Plates were incubated for 1 h at 37°C. Values were determined by reading fluorescence on a fluorometric plate reader (Spectramax Gemini XPS; Molecular Devices) with an excitation wavelength of 360 nm and an emission wavelength of 460 nm. Calculation of net fluorescence included the subtraction of a blank consisting of buffer containing no NAD⁺.

RNA interference and rescue expression of DBC1. Cells were transfected with 100 nM control small interfering RNA (siRNA) or 100 nM DBC1 custom siRNA (5'-CAGCUUGCAUGACUACUUUUU-3') or hMOF SMARTpool siRNAs (Dharmacon) using RNAiMAX (Invitrogen) according to instructions from the supplier. After 48 h of transfection, cells were treated with etoposide (50 μ M) or ionizing radiation (IR) (10 Gy) and analyzed for mRNA or protein level. The siRNA target sequence in pBABE-FLAG-DBC1 was mutated to 5'ACCAGCTTGACGATTACTTT (the underlined sequence contains mutations that prevent siRNA binding without affecting protein coding potential) to create siRNA-resistant DBC1, followed by introduction of 112- and 215-dR and 112- and 215-dQ (i.e., double arginine [dR] and double glutamine [dQ] substitutions for K112 and K215).

Luciferase reporter assay. Cells (50,000 per well) were cultured in 24-well plates and transfected with a mixture containing 50 ng p53-responsive luciferase reporter plasmid (BP100-luc), 5 ng cytomegalovirus (CMV)-*lacZ* plasmid, 100 ng DBC1 expression plasmids, and/or SirT1 expression plasmid. Transfection was achieved using Lipofectamine Plus reagents (Invitrogen). Cell lysate was analyzed for luciferase and β -galactosidase (β -Gal) expression after 24 h. The ratio of luciferase to β -Gal activity was used as an indicator of transcription activity.

Immunofluorescence staining. Cells cultured on chamber slides were fixed with 4% paraformaldehyde for 5 min at room temperature, blocked with phosphate-buffered saline (PBS) plus 10% normal goat serum (NGS) for 20 min, and incubated with primary antibody in PBS with 10% NGS for 2 h. The slides were washed with PBS plus 0.1% Triton X-100, incubated with fluorescein isothiocyanate (FITC)-conjugated goat anti-mouse and/or rhodamine-conjugated goat anti-rabbit IgG in PBS plus 10% NGS for 2 h, washed with PBS plus 0.1% Triton X-100, and mounted.

Colony formation assay. The colony formation assay was performed as described previously (38). Briefly, 5,000 cells were seeded in a 10-cm plate in triplicate, incubated for 8 h to allow attachment, treated with ionizing radiation (IR), and cultured for 7 to 10 days. After incubation, cells were washed with PBS, stained with 0.5% crystal violet for 1 min at 23°C, washed with PBS, and photographed for colony density. To quantify surviving cells, the crystal violet in stained colonies was extracted by

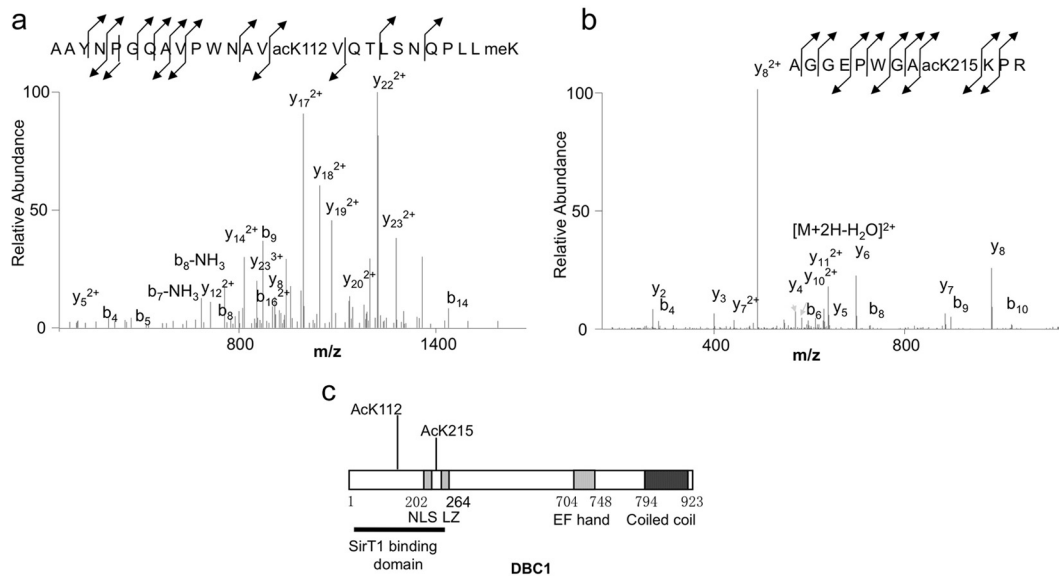


FIG 1 DBC1 is modified by acetylation. (a) Myc-tagged DBC1 was transiently transfected into H1299 cells and purified by immunoprecipitation using Myc antibody. Acetylation of DBC1 was analyzed by tandem mass spectrometry. Acetylation of lysine 112 was detected in the peptide sequence AAYNPGQAVPWNAV(AcK)112VQTLNSNQPLL(MeK), matched with a Sequest Xcorr value of 2.5. (b) Acetylation of lysine 215 was observed in the peptide sequence AGGEPWGA(AcK)215KPR, which matched sequence with a Sequest Xcorr value of 3.05. Ac, acetylation; me, methylation. (c) Diagram of DBC1 domains and locations of acetylation lysines.

incubation with 10% acetic acid for 20 min, and absorbance at 590 nm was measured.

Comet assay. Neutral comet assays were performed according to the manufacturer's suggestions (Trevigen). Cells were lysed, mixed with low-melting-point agarose gel, spread on slides, and subjected to electrophoresis in neutral Tris-borate-EDTA (TBE) buffer at 21 V for 30 min (Fisher Midi-horizontal system FB-SB-1316 with a 27-cm-wide tank). The nuclei on slides were stained with SYBR green and visualized by microscopy. Images were captured and measured by an automated comet assay analysis system (HCSA 2.3.3; Loats Associates). The extent of DNA strand break (DSB) damage was represented by the parameter of tail moment, a combination of the amount of DNA and the length in the tail of the comet. At least 100 cells were measured for each sample, and each experiment was repeated twice.

Apoptosis assay. Cells stably expressing siRNA-resistant DBC1 wild type or the DBC1-dR and DBC1-dQ mutants were transfected with DBC1 siRNA. After 2 days, cells were treated with etoposide (20 to 50 μ M) or ionizing radiation (10 Gy). After an additional 24 to 48 h, cells were washed with PBS, fixed in 4% paraformaldehyde at room temperature, and then stained with 2 μ g/ml DAPI (4',6-diamidino-2-phenylindole). The number of apoptotic cells with a fragmented nuclear morphology typical of apoptosis was analyzed by fluorescence microscopy and scored in at least 500 cells per sample by an analyst blinded to the sample groups.

Statistical analysis. Data are expressed as means \pm standard deviations (SD). Statistical analysis was performed using SPSS software (release 13.0; SPSS, Inc.). The difference between two groups was analyzed by the Student's *t* test. A value of *P* < 0.05 was considered statistically significant.

RESULTS

DBC1 is modified by hMOF-mediated acetylation. To determine whether DBC1 is regulated by acetylation, Myc-tagged DBC1 was purified from transfected H1299 cells and analyzed by mass spectrometry (Fig. 1a and b). The results suggested that K112 and K215 in the N-terminal region were modified by acetylation (Fig. 1c). These two residues are located in a highly conserved region of DBC1 from different species. To identify the acetyltransferase that

promotes DBC1 acetylation, candidate histone acetyltransferases (HATs) were cotransfected with Myc-tagged DBC1, followed by Myc immunoprecipitation (IP) and Western blotting using anti-acetyllysine antibody. Of the 5 HATs tested (hMOF, Tip60, p300, PCAF, and HBO1), only hMOF promoted strong acetylation of DBC1 (Fig. 2a). Two catalytically dead mutants of hMOF did not promote DBC1 acetylation (Fig. 2b). Double arginine (dR) (Fig. 2c) or double glutamine (dQ) substitution for K112 and K215 eliminated most of the acetylation signal (data not shown), whereas single arginine substitution for K112 or K215 each caused only moderate reduction of DBC1 acetylation by hMOF (Fig. 2c), suggesting that hMOF acetylates both K112 and K215.

To confirm that hMOF can directly acetylate DBC1, GST-DBC1-1–240 was used as a substrate in an *in vitro* acetylation assay by hMOF immunoprecipitated from transfected H1299 cells. Purified hMOF promoted the acetylation of the DBC1-1–240 fragment but did not acetylate DBC1-1–240 containing the K112R K215R double substitution (Fig. 2d), suggesting that hMOF can acetylate DBC1 *in vitro* on K112 and K215. To test whether endogenous hMOF is required for DBC1 acetylation, U2OS cells stably expressing Myc-DBC1 were treated with hMOF siRNA, and Myc-DBC1 was immunoprecipitated and probed with antiacetyllysine antibody. Knockdown of hMOF significantly reduced the level of DBC1 acetylation (Fig. 2e). Ectopic expression of FLAG-hMOF also increased the acetylation level of endogenous DBC1 (Fig. 2f). These results suggest that DBC1 is a nonhistone substrate of hMOF.

SirT1 inhibits DBC1 acetylation by hMOF. Since SirT1 interacts with both DBC1 and hMOF, its effect on hMOF-mediated DBC1 acetylation was tested. The result showed that overexpression of SirT1 (but not the catalytically inactive SirT1-363A) abrogated DBC1 acetylation by hMOF, suggesting that SirT1 may regulate DBC1 acetylation (Fig. 3a). Treatment of U2OS-Myc-DBC1 stably transfected cells with SirT1 inhibitor EX-527 also increased

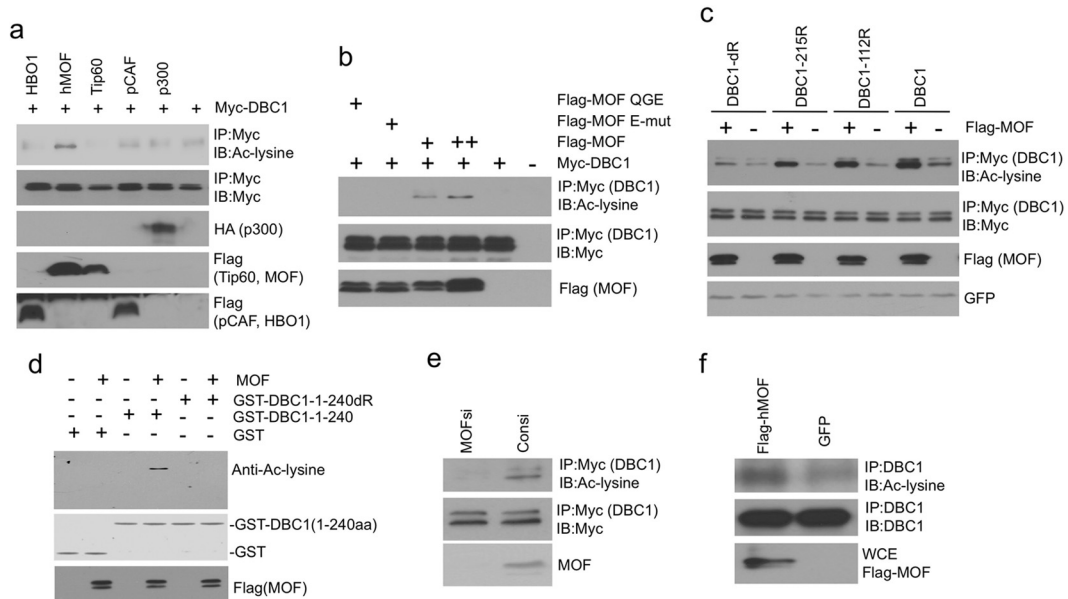


FIG 2 DBC1 is modified by hMOF-mediated acetylation. (a) H1299 cells were transfected with the indicated plasmids for 48 h. Myc-DBC1 was immunoprecipitated and probed using antiacetyllysine antibody. The membrane was stripped and reprobed with Myc antibody to confirm a uniform DBC1 loading level. IB, Western immunoblotting. (b) H1299 cells were transfected with the indicated hMOF catalytic mutants for 48 h. Myc-DBC1 was immunoprecipitated and probed using antiacetyllysine antibody. (c) H1299 cells were transfected with DBC1 lysine-to-arginine substitution mutants for 48 h (K112R, K215R, or K112R K215R). Myc-DBC1 was immunoprecipitated and probed using antiacetyllysine antibody. (d) GST-DBE1-1-240 with wild-type sequence or the 112R 215R double substitution was incubated with FLAG-hMOF immunopurified from transfected H1299 cells in the presence of acetyl-CoA and analyzed by Western blotting using the indicated antibodies. The levels of the GST fusion proteins are shown in the bottom panel as stained by Coomassie blue. (e) The U2OS-Myc-DBC1 stable cell line was treated with hMOF siRNA for 48 h. The DBC1 acetylation level was analyzed by Myc IP followed by antiacetyllysine Western blotting. (f) U2OS cells were transfected with hMOF for 48 h. The endogenous DBC1 acetylation level was analyzed by DBC1 IP followed by antiacetyllysine Western blotting. WCE, whole-cell extract.

the level of DBC1 acetylation by endogenous acetylase or by transfected hMOF (Fig. 3b). Treatment with TSA did not affect DBC1 acetylation, suggesting that class III HDACs were responsible for the deacetylation of DBC1 (data not shown). Among the seven mammalian sirtuins, only SirT1 showed robust activity in suppressing DBC1 acetylation by hMOF in the transfection assay (Fig. 3c). These results suggest that SirT1 is a major regulator of the DBC1 acetylation level in cells.

Acetylation of DBC1 inhibits binding to SirT1. Our previous deletion mapping showed that the fragment from positions 1 to

240 of DBC1 was sufficient to mediate strong binding to SirT1 and SUV39H1 *in vitro*; deletion of residues 1 to 107 of DBC1 significantly reduced SirT1 and SUV39H1 binding *in vivo* (23). Therefore, the DBC1 fragment from positions 1 to 240 contains a strong SirT1 binding domain separate from the previously reported SirT1 binding site at the leucine zipper (positions 243 to 264) (19). In the cotransfection assay, mutagenesis of K112 and K215 to R (to block acetylation) slightly increased DBC1 binding to SirT1, whereas mutation to Q (to mimic acetylation) strongly inhibited SirT1 binding (Fig. 4a). Expression of exogenous hMOF inhibited

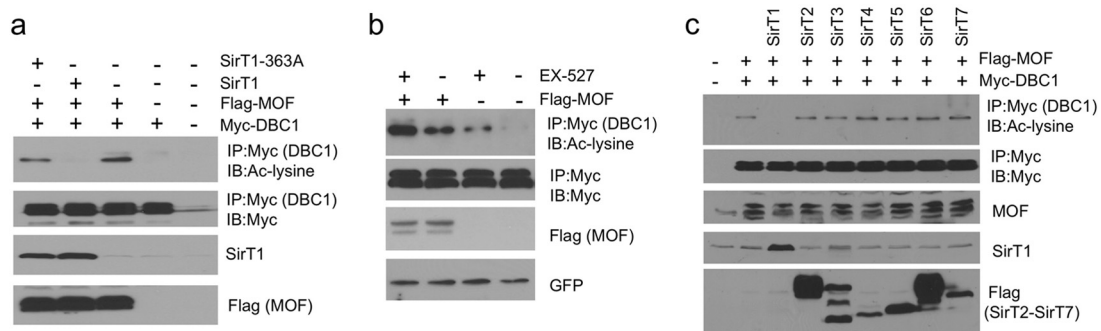


FIG 3 SirT1 inhibits DBC1 acetylation by hMOF. (a) H1299 cells were transfected with the indicated plasmids for 48 h. The DBC1 acetylation level was analyzed by IP and Western blotting. Overexpression of SirT1 (but not the catalytically inactivated SirT1-363A mutant) abrogated DBC1 acetylation by hMOF. (b) U2OS cells stably expressing Myc-DBC1 were transfected with hMOF or empty vector for 40 h, treated with 2 μ M SirT1 inhibitor EX-527 for 6 h, and analyzed for DBC1 acetylation by IP and Western blotting. EX-527 increased the endogenous and ectopic DBC1 acetylation level. (c) H1299 cells were transfected with sirtuin family homologs for 48 h, and DBC1 acetylation was analyzed by IP and Western blotting. SirT1 specifically inhibited hMOF-dependent acetylation of DBC1.

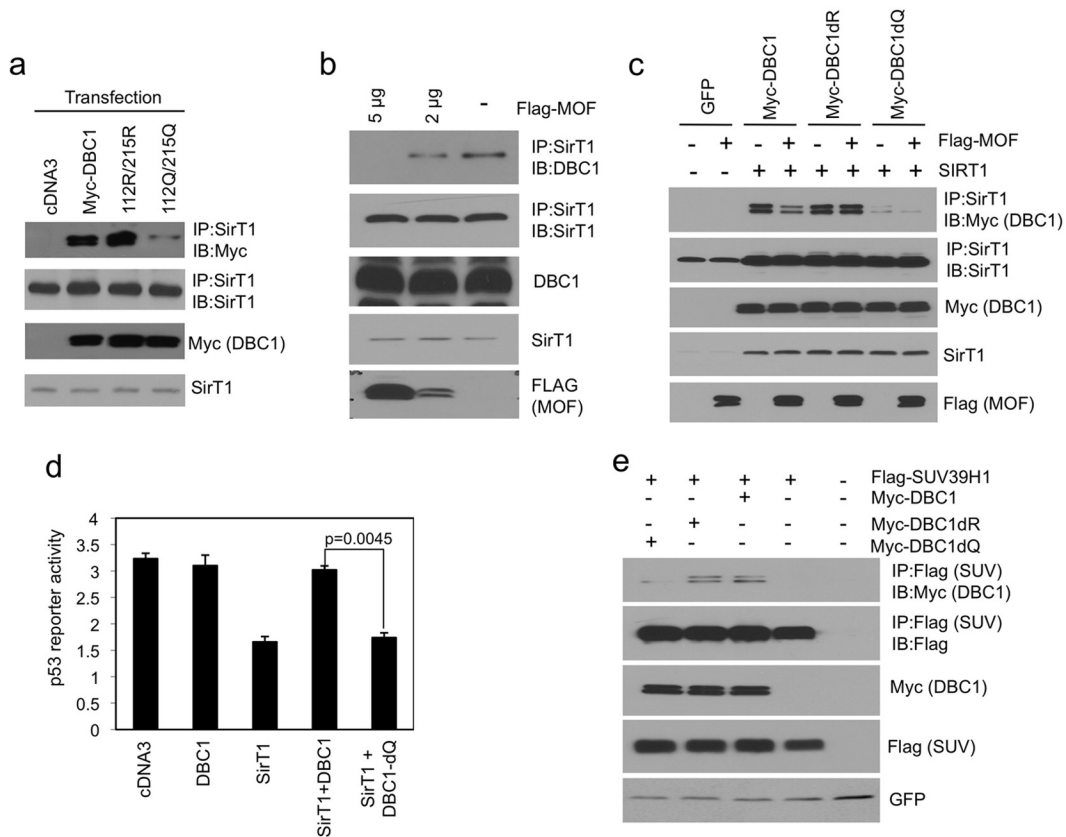


FIG 4 Acetylation of DBC1 inhibits binding to SirT1. (a) H1299 cells were transfected with the indicated Myc-DBC1 mutants for 48 h, and DBC1 binding to endogenous SirT1 was analyzed by IP and Western blotting. The DBC1 double Q mutation (to mimic acetylation) strongly inhibited SirT1 binding. (b) H1299 cells were transiently transfected with hMOF and analyzed for endogenous SirT1-DBC1 binding by IP and Western blotting. Endogenous SirT1-DBC1 binding was inhibited by ectopic hMOF expression. (c) H1299 cells were transfected with SirT1 and DBC1 mutants in the presence or absence of hMOF. The binding between exogenous SirT1 and DBC1 was analyzed by IP and Western blotting. The DBC1-dR mutant was resistant to inhibition by hMOF. (d) U2OS cells were transfected with SirT1 and the p53-responsive BP100-luciferase reporter as a readout of endogenous p53 activity. The ability of DBC1 to block p53 inhibition by SirT1 was analyzed by luciferase assay. DBC1-dQ (112Q 215Q) lost its inhibitory effect on SirT1. (e) H1299 cells were transfected with SUV39H1 and DBC1 mutants. DBC1-SUV39H1 binding was analyzed by IP and Western blotting. DBC1-SUV39H1 interaction was inhibited by 112Q 215Q substitution.

the interaction between endogenous SirT1 and DBC1 in a dose-dependent manner in H1299 cells (Fig. 4b). In the cotransfection assay, the binding between DBC1 and SirT1 was inhibited by hMOF, but DBC1-112R/215R binding to SirT1 was not inhibited by hMOF (Fig. 4c). In a luciferase reporter assay, SirT1 expression suppressed the activity of a p53-responsive reporter by 50%. Wild-type DBC1 coexpression restored p53 activity, whereas the SirT1 binding-deficient mutant DBC1-dQ did not rescue p53 from SirT1-mediated inhibition (Fig. 4d). Consistent with the previous finding that positions 1 to 240 of DBC1 are also involved in binding to SUV39H1 (23), the ability of DBC1 to bind SUV39H1 was inhibited by 112Q and 215Q substitution (Fig. 4e). These results suggest that acetylation of DBC1 alters the conformation or surface charge of the N-terminal domain and inhibits the binding to SirT1.

hMOF abrogates the ability of DBC1 to inhibit SirT1. To further test whether hMOF regulates the ability of DBC1 to inhibit SirT1, the p53 K382 acetylation level was used as readout of SirT1 activity *in vivo*. In the *in vivo* assay, p53 K382 acetylation by p300 was suppressed by SirT1. DBC1 expression restored the p53 acetylation level, which was abrogated by hMOF (Fig. 5a). Furthermore, the ability of DBC1-dR to rescue p53 acetylation was not

affected by hMOF. As expected, DBC1-dQ failed to inhibit SirT1 function and did not restore p53 acetylation, consistent with its deficiency in SirT1 binding (Fig. 5a). In an *in vitro* SirT1 activity assay using acetylated p53 peptide as the substrate, DBC1 coexpression inhibited the deacetylase activity of SirT1, whereas the DBC1-dQ mutant did not inhibit SirT1 (Fig. 5b). By acetylating DBC1, endogenous hMOF expression is predicted to help maintain high SirT1 activity and reduce the p53 K382 acetylation level. As expected, knockdown of endogenous hMOF in U2OS cells increased the p53 K382 acetylation level and increased p21 expression after IR and etoposide treatments (Fig. 5c). These results showed that hMOF regulates the ability of DBC1 to inhibit SirT1 through acetylation of DBC1.

DNA damage inhibits DBC1-hMOF binding and DBC1 acetylation. Since acetyltransferases often show detectable interaction with substrates, we tested whether hMOF can directly interact with DBC1. We performed immunoprecipitation of endogenous hMOF and detected the coprecipitation of endogenous DBC1 using two different cell lines (Fig. 6a). Cotransfection of ectopic hMOF and DBC1 also resulted in strong complex formation, which allowed mapping analyses using hMOF and DBC1 deletion mutants. The results showed that DBC1 binds to the central re-

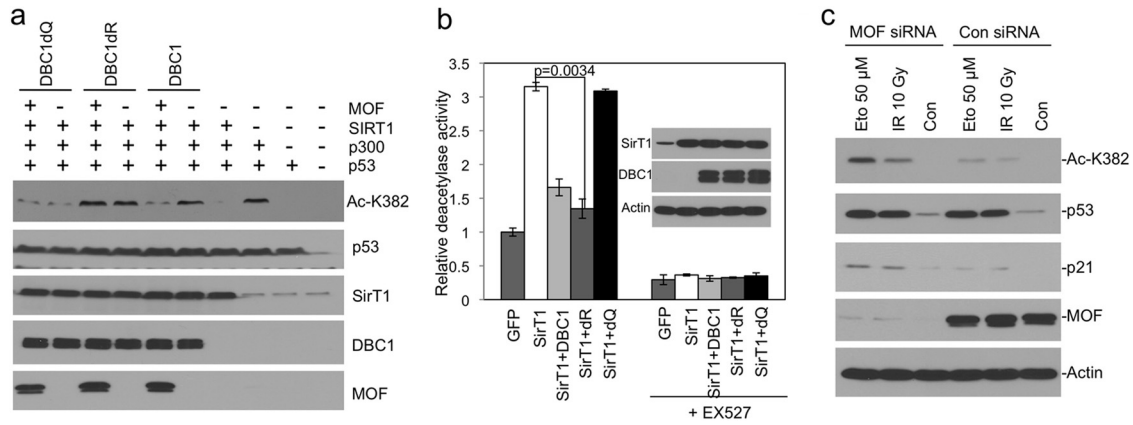


FIG 5 hMOF abrogates the ability of DBC1 to inhibit SirT1. (a) H1299 cells were transfected with the indicated plasmids. p53 acetylation by p300 was analyzed using Ac-K382-specific antibody. hMOF acetylation of DBC1 abrogates the ability of DBC1 to inhibit SirT1. (b) H1299 cells were transfected with the indicated plasmids for 48 h and assayed for SirT1 activity using a fluorometric kit. DBC1 acetylation-mimetic substitution abrogated the ability to inhibit SirT1 deacetylase activity. (c) U2OS cells were transfected with hMOF siRNA for 48 h and treated with 50 μ M etoposide or 10 Gy gamma irradiation for 2 h. The p53 acetylation level and induction of p21 expression were analyzed by Western blotting. Knockdown of endogenous hMOF increased p53 K382 acetylation and p21 expression after DNA damage.

gion of hMOF that overlaps with the MYST acetyltransferase catalytic domain (Fig. 6b and c). Using a panel of DBC1 deletion mutants, the hMOF binding site on DBC1 was mapped to the fragment from positions 1 to 240 that contains the acetylation sites

(Fig. 6d and e). Further immunofluorescence staining confirmed that both hMOF and DBC1 colocalized in the nucleus (data not shown). hMOF-DBC1 binding (but not that of the DBC1-dR mutant) was inhibited by SirT1 (Fig. 6f). This is consistent with the

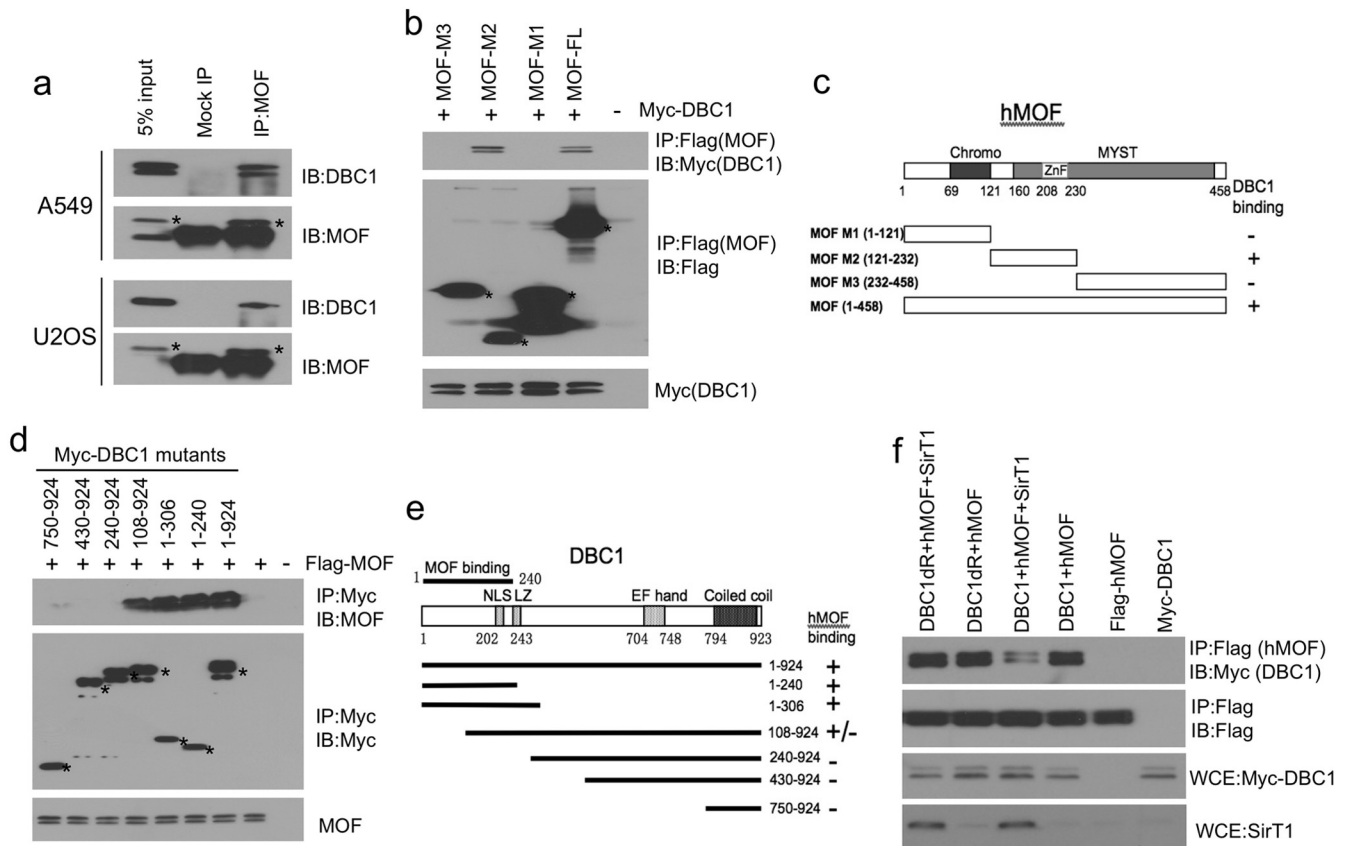


FIG 6 Binding domain mapping of DBC1 and MOF. (a) A549 and U2OS cells were analyzed by hMOF IP followed by DBC1 Western blotting to detect the interaction between endogenous DBC1 and hMOF. The hMOF bands are marked by asterisks. (b) H1299 cells were transfected with DBC1 with hMOF deletion mutants. DBC1 binding to hMOF mutants was analyzed by IP and Western blotting. Asterisks indicate the location of hMOF mutant bands. (c) Diagram of hMOF and summary of results in panel b. (d) H1299 cells were transfected with hMOF and DBC1 deletion mutants. hMOF binding to DBC1 mutants was analyzed by IP and Western blotting. Asterisks indicate the locations of DBC1 mutant bands. (e) Diagram of DBC1 and summary of results in panel d. (f) H1299 cells were transfected with the indicated plasmids, and the effect of SirT1 on hMOF-DBC1 binding was analyzed by IP and Western blotting.

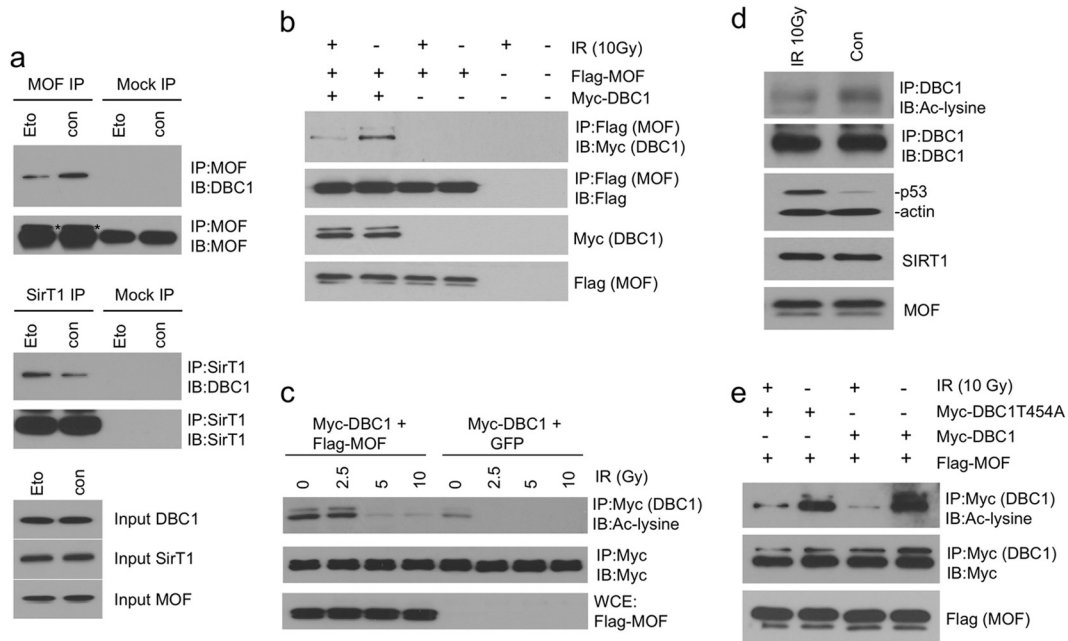


FIG 7 DNA damage inhibits DBC1-hMOF binding and DBC1 acetylation. (a) U2OS cells were treated with 50 μ M etoposide (Eto) for 6 h and subjected to IP and Western blot analysis to detect the binding between endogenous hMOF-DBC1 (top panels) and SirT1-DBC1 (middle panels). DNA damage reduces the endogenous DBC1-hMOF binding and increases DBC1-SirT1 binding. con, control. (b) U2OS cells were transfected with indicated plasmids for 40 h and exposed to 10 Gy IR for 4 h. The binding between ectopic DBC1 and hMOF was analyzed by IP and Western blotting. (c) U2OS cells stably expressing Myc-DBC1 were transfected with or without hMOF for 40 h, treated with IR for 4 h, and analyzed for DBC1 acetylation level by IP and Western blotting. DNA damage reduces the acetylation of Myc-DBC. (d) U2OS cells were exposed to 10 Gy IR for 4 h and analyzed for the endogenous DBC1 acetylation level by IP and Western blotting. DNA damage reduces the endogenous acetylation of DBC. (e) H1299 cells were transfected with indicated plasmids, treated with IR, and analyzed for the DBC1 acetylation level. The DBC1-454A mutation did not prevent IR inhibition of DBC1 acetylation.

mapping of the hMOF binding site to the DBC1 region from 1 to 240 and suggests that DBC1 acetylation promotes DBC1-hMOF binding and inhibits DBC1-SirT1 binding.

Next, we tested whether hMOF-DBC1 interaction is regulated by stress. Treatment with the DNA-damaging agent etoposide reduced the binding between endogenous hMOF and DBC1 (Fig. 7a, top panels). Correspondingly, DBC1 coprecipitation with SirT1 was increased after DNA damage, as reported previously (Fig. 7a, middle panels). The binding between transfected hMOF and DBC1 was also significantly inhibited by gamma irradiation (Fig. 7b). Consistent with reduced hMOF-DBC1 binding, the acetylation level of stably expressed Myc-DBC1 in U2OS cells was reduced after irradiation (Fig. 7c). The acetylation of endogenous DBC1 was also reduced after IR, although the signal was less definitive than that in assays using ectopic DBC1 due to limited sensitivity (Fig. 7d). DNA damage has been shown to induce phosphorylation of DBC1 on T454, which in turn increases binding to SirT1. We found that the ability of IR to inhibit DBC1 acetylation was not affected by mutation of the ATM phosphorylation site (T454A) on DBC1 (Fig. 7e), suggesting that T454 phosphorylation was not required for the regulation of DBC1 acetylation by DNA damage.

ATM mediates DNA damage inhibition of DBC1-hMOF binding. Since ATM is required for promoting SirT1-DBC1 binding after DNA damage (25), it may act partly through regulating hMOF-DBC1 interaction. Consistent with this notion, treatment with the ATM-specific inhibitor KU-55933 prevented the disruption of hMOF-DBC1 binding by IR (Fig. 8a). Unlike full-length hMOF, the central fragment of hMOF (MOF-M2) interacted with

DBC1 efficiently, but the binding was not inhibited by IR (Fig. 8b), suggesting that the N- or C-terminal region missing in the M2 construct was required for regulation by ATM.

To further test the mechanism by which DNA damage regulates hMOF-DBC1 interaction, an *in vitro* binding assay was employed. DBC1 and hMOF were transfected into U2OS cells separately and treated with DNA damage. The cell extracts were mixed, and the formation of DBC1-hMOF complex *in vitro* was analyzed by IP and Western blotting. The result suggested that when hMOF was provided from cells treated with IR, hMOF-DBC1 binding was reduced. In contrast, DBC1 from IR-treated cells showed no change in hMOF binding efficiency (Fig. 8c). Therefore, modification of hMOF after DNA damage appeared to be responsible for inhibition of DBC1-hMOF complex formation. The C terminus of hMOF contains several potential ATM phosphorylation sites (SQ and TQ). It remains to be determined whether hMOF is regulated directly by ATM-mediated phosphorylation.

DBC1 acetylation reduces its cell death-promoting function. The ability of SirT1 to deacetylate p53 and other factors has an antiapoptotic effect after DNA damage. To test the role of DBC1 acetylation in regulating cell fate after DNA damage, U2OS cells were treated with IR and analyzed for cell death by trypan blue exclusion assay. Transfection of wild-type DBC1 increased the level of cell death after IR by 2-fold; the SirT1 binding-defective DBC1-dQ mutant was not able to promote cell death (Fig. 9a). SirT1 has been implicated in promoting DNA repair (3). When analyzed using the comet assay, the level of DNA strand breaks after etoposide treatment was increased in DBC1-transfected cells, consistent with low SirT1 activity and compromised repair effi-

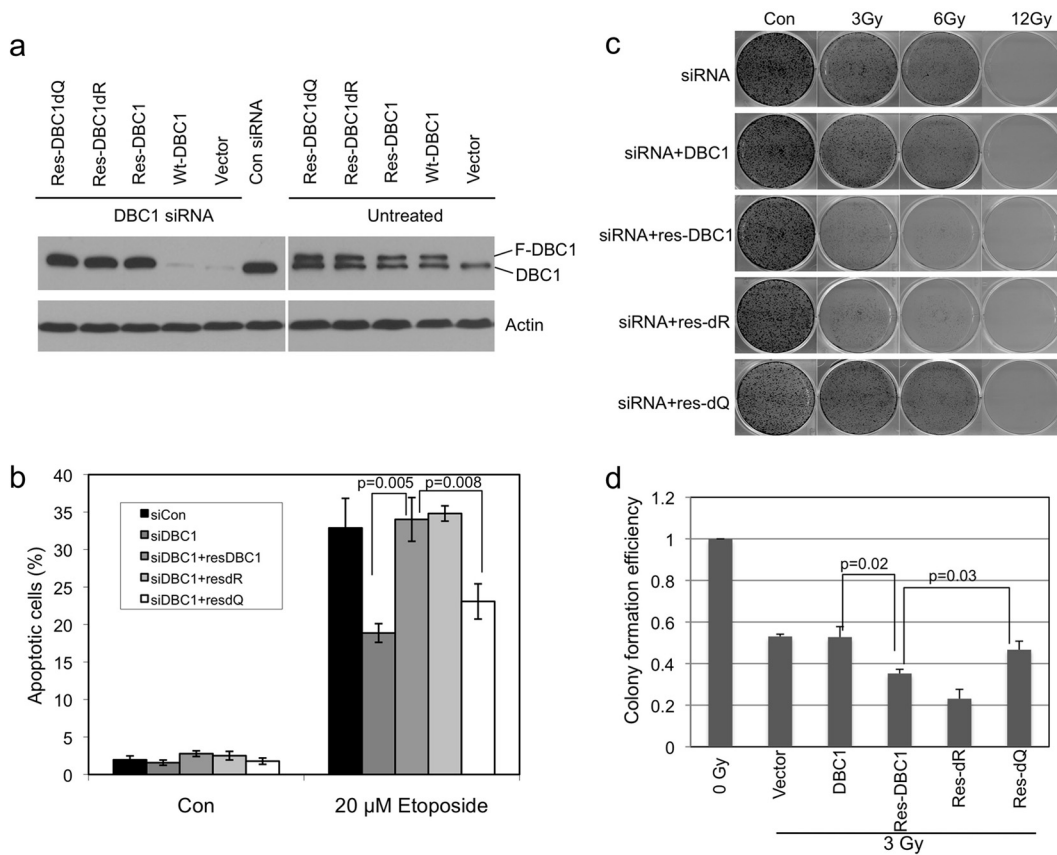


FIG 10 Functional significance of DBC1 acetylation. (a) A549 cells stably expressing vector, siRNA-resistant pBABE-Flag-DBC1 (res-wild type [WT], res-dR, or res-dQ) were transfected two times with DBC1 siRNA and analyzed by Western blotting using DBC1 antibody to confirm depletion of endogenous DBC1 (lower band) and persistent expression of ectopic FLAG-DBC1 mutants (upper band). (b) Cells as in panel a were treated with 20 μ M etoposide for 48 h, and the apoptotic population was determined. (c) A549 cells stably expressing siRNA-resistant DBC1 mutants were treated with DBC1 siRNA for 48 h to deplete endogenous DBC1, treated with IR, and cultured for 14 days to determine colony formation efficiency. (d) Quantification of stained cells in panel c by dye extraction and optical density measurement.

is necessary for downregulation of SirT1 activity and ensuring commitment to cell death. Forced sustainment of DBC1 acetylation (as mimicked by expression of the res-DBC1-dQ) after DNA damage leads to high-level SirT1 activity that blocks induction of cell death.

DISCUSSION

DBC1 is an important SirT1 binding partner and an inhibitor of SirT1 deacetylase function. Given the many roles of SirT1 in regulating cellular response to nutrient and genotoxic stress, DBC1 function is expected to be tightly regulated by different stress signaling pathways. Recent studies showed that ATM-mediated phosphorylation of DBC1 on T454 after DNA damage stimulates binding to SirT1, inhibiting SirT1 activity and promoting cell death (25, 26). The findings reported here suggest that DBC1 function is also regulated by acetylation of two N-terminal residues, K112 and K215. We demonstrate that the MYST family enzyme hMOF is a bona fide regulator of DBC1. By acetylating K112 and K215 on the N-terminal SirT1 binding domain of DBC1, hMOF disrupts DBC1-SirT1 interaction and increases the activity of SirT1. A recent study also independently identified four acetylation sites on DBC1, including the two sites found in our study (39).

Interestingly, the DBC1 acetylation level is downregulated after DNA damage, possibly through ATM-dependent inhibition of DBC1-hMOF binding. Downregulation of DBC1 acetylation after DNA damage is consistent with the increased DBC1-SirT1 complex formation reported in previous studies (19, 25). Phosphorylation of DBC1 on T454 and deacetylation of K112 and K215, both dependent on the activity of ATM, may synergistically enhance SirT1 binding. ATM phosphorylation of T454 has been shown to create a secondary SirT1 binding site to stabilize the DBC1-SirT1 complex. Our results suggest that ATM is also required for promotion of modification of hMOF and reduction of its binding affinity for DBC1. Consequently, ATM inhibits hMOF-mediated acetylation of the DBC1 N-terminal domain, which should also lead to enhanced DBC1-SirT1 binding. Whether hMOF is a direct phosphorylation target of ATM is currently unknown. It remains to be determined whether DBC1 acetylation is regulated by other signaling pathways in addition to genotoxic stress.

The activity of hMOF is suppressed by SirT1-mediated deacetylation of residues at the catalytic domain (36). Our present results showed that SirT1 can suppress DBC1 acetylation by hMOF. The N-terminal domain of DBC1 is involved in binding to both SirT1 and hMOF. It is unclear whether SirT1 acts by direct deacetylation of DBC1, deacetylation and inactivation of hMOF,

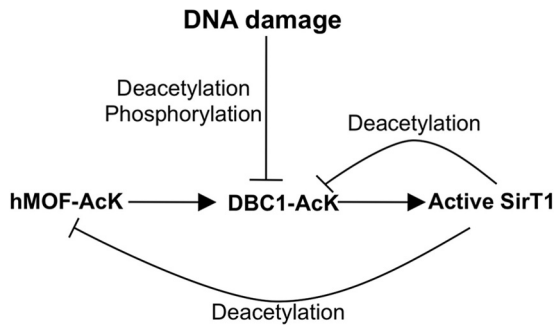


FIG 11 A model of regulation between hMOF-DBC1-SirT1 following DNA damage. hMOF acetylates DBC1 and reduces its SirT1 binding affinity, leading to increased SirT1 activity. SirT1 downregulates DBC1 and hMOF acetylation levels, thus forming two negative-feedback loops that limit its own basal activity. DNA damage activation of ATM blocks hMOF-DBC1 and hMOF-SirT1 interactions and inhibits DBC1 acetylation, thus disrupting both negative-feedback loops and activating SirT1. These feedback mechanisms help maintain cellular homeostasis while providing the ability to respond to DNA damage by activating SirT1, promoting DNA repair, and suppressing apoptosis.

competition with hMOF for binding to DBC1, or a combination of all three mechanisms *in vivo*. Irrespective of the details, SirT1-mediated suppression of DBC1 acetylation level suggests the presence of a negative-feedback mechanism that limits the activity of SirT1 (Fig. 11), since deacetylation of DBC1 promotes formation of inactive DBC1-SirT1 complex.

It is possible that hMOF acetylation of DBC1 has additional functions in the feedback regulation of hMOF itself. hMOF is a major acetylase for H4 K16 and is important for efficient DNA damage repair. SirT1 deacetylates H4 K16 and may antagonize the function of hMOF. During homeostatic conditions, hMOF constantly acetylates DBC1 and activates SirT1, creating a negative-feedback loop to limit its own activity. After DNA damage, ATM acts as the master regulator to suppress DBC1 acetylation and inhibit SirT1 activity, thus preventing deacetylation of H4 K16. DNA damage also disrupts the SirT1-hMOF interaction and promotes hyperacetylation and activation of hMOF, which enhances its DNA repair and apoptosis functions (36). ATM inhibition of DBC1 acetylation by hMOF provides an additional mechanism that would facilitate hMOF activation and promote DNA strand break repair.

In summary (Fig. 11), we showed that acetylation of DBC1 by hMOF regulates its SirT1 binding affinity and cell death-promoting function. We also established a novel signaling mechanism that links DBC1 function to DNA damage response. The antagonistic effects of SirT1 and hMOF in regulating the acetylation of DBC1 and histone H4 K16 suggest the presence of multiple negative-feedback loops that maintain an intricate balance between these enzymes. These interactions constitute a small part of a network necessary for maintaining cellular homeostasis while providing the ability to rapidly respond to genome damage and changes in metabolism.

ACKNOWLEDGMENTS

We thank the Moffitt Molecular Genomics Core for DNA sequence analyses, Analytic Microscopy Core for image quantification, and Moffitt Proteomics Core for protein mass spectrometric analyses.

H. Zheng is supported by a postdoctoral fellowship from the Florida Department of Health James and Esther King Biomedical Research Pro-

gram. This work is supported by grants from the National Institutes of Health to J. Chen (CA141244, CA109636, and CA121291).

We declare that we have no conflicts of interest.

REFERENCES

- Imai S, Armstrong CM, Kaerberlein M, Guarente L. 2000. Transcriptional silencing and longevity protein Sir2 is an NAD-dependent histone deacetylase. *Nature* 403:795–800.
- Rodgers JT, Lerin C, Haas W, Gygi SP, Spiegelman BM, Puigserver P. 2005. Nutrient control of glucose homeostasis through a complex of PGC-1 α and SIRT1. *Nature* 434:113–118.
- Yuan Z, Zhang X, Sengupta N, Lane WS, Seto E. 2007. SIRT1 regulates the function of the Nijmegen breakage syndrome protein. *Mol. Cell* 27:149–162.
- Zhou Y, Schmitz KM, Mayer C, Yuan X, Akhtar A, Grummt I. 2009. Reversible acetylation of the chromatin remodelling complex NoRC is required for non-coding RNA-dependent silencing. *Nat. Cell Biol.* 11:1010–1016.
- Murayama A, Ohmori K, Fujimura A, Minami H, Yasuzawa-Tanaka K, Kuroda T, Oie S, Daitoku H, Okuwaki M, Nagata K, Fukamizu A, Kimura K, Shimizu T, Yanagisawa J. 2008. Epigenetic control of rDNA loci in response to intracellular energy status. *Cell* 133:627–639.
- Fan W, Luo J. 2010. SIRT1 regulates UV-induced DNA repair through deacetylating XPA. *Mol. Cell* 39:247–258.
- Wang RH, Sengupta K, Li C, Kim HS, Cao L, Xiao C, Kim S, Xu X, Zheng Y, Chilton B, Jia R, Zheng ZM, Appella E, Wang XW, Ried T, Deng CX. 2008. Impaired DNA damage response, genome instability, and tumorigenesis in SIRT1 mutant mice. *Cancer Cell* 14:312–323.
- Vaquero A, Scher M, Lee D, Erdjument-Bromage H, Tempst P, Reinberg D. 2004. Human SirT1 interacts with histone H1 and promotes formation of facultative heterochromatin. *Mol. Cell* 16:93–105.
- Luo J, Nikolaev AY, Imai S, Chen D, Su F, Shiloh A, Guarente L, Gu W. 2001. Negative control of p53 by Sir2 α promotes cell survival under stress. *Cell* 107:137–148.
- Vaziri H, Dessain SK, Ng Eaton E, Imai SI, Frye RA, Pandita TK, Guarente L, Weinberg RA. 2001. hSIR2(SIRT1) functions as an NAD-dependent p53 deacetylase. *Cell* 107:149–159.
- Cohen HY, Miller C, Bitterman KJ, Wall NR, Hekking B, Kessler B, Houtz KT, Gorospe M, de Cabo R, Sinclair DA. 2004. Calorie restriction promotes mammalian cell survival by inducing the SIRT1 deacetylase. *Science* 305:390–392.
- Motta MC, Divecha N, Lemieux M, Kamel C, Chen D, Gu W, Bultsma Y, McBurney M, Guarente L. 2004. Mammalian SIRT1 represses forkhead transcription factors. *Cell* 116:551–563.
- Liou GG, Tanny JC, Kruger RG, Walz T, Moazed D. 2005. Assembly of the SIR complex and its regulation by O-acetyl-ADP-ribose, a product of NAD-dependent histone deacetylation. *Cell* 121:515–527.
- Vaquero A, Scher M, Erdjument-Bromage H, Tempst P, Serrano L, Reinberg D. 2007. SIRT1 regulates the histone methyl-transferase SUV39H1 during heterochromatin formation. *Nature* 450:440–444.
- Revollo JR, Grimm AA, Imai S. 2004. The NAD biosynthesis pathway mediated by nicotinamide phosphoribosyltransferase regulates Sir2 activity in mammalian cells. *J. Biol. Chem.* 279:50754–50763.
- Nasrin N, Kaushik VK, Fortier E, Wall D, Pearson KJ, de Cabo R, Bordone L. 2009. JNK1 phosphorylates SIRT1 and promotes its enzymatic activity. *PLoS One* 4:e8414. doi:10.1371/journal.pone.0008414.
- Kim EJ, Kho JH, Kang MR, Um SJ. 2007. Active regulator of SIRT1 cooperates with SIRT1 and facilitates suppression of p53 activity. *Mol. Cell* 28:277–290.
- Zhao W, Kruse JP, Tang Y, Jung SY, Qin J, Gu W. 2008. Negative regulation of the deacetylase SIRT1 by DBC1. *Nature* 451:587–590.
- Kim JE, Chen J, Lou Z. 2008. DBC1 is a negative regulator of SIRT1. *Nature* 451:583–586.
- Gray KA, Daugherty LC, Gordon SM, Seal RL, Wright MW, Bruford EA. 2013. Genenames.org: the HGNC resources in 2013. *Nucleic Acids Res.* 41:D545–D552.
- Escande C, Chini CC, Nin V, Dykhouse KM, Novak CM, Levine J, van Deursen J, Gores GJ, Chen J, Lou Z, Chini EN. 2010. Deleted in breast cancer-1 regulates SIRT1 activity and contributes to high-fat diet-induced liver steatosis in mice. *J. Clin. Invest.* 120:545–558.
- Hamaguchi M, Meth JL, von Klitzing C, Wei W, Esposito D, Rodgers L, Walsh T, Welch P, King MC, Wigler MH. 2002. DBC2, a candidate

- for a tumor suppressor gene involved in breast cancer. *Proc. Natl. Acad. Sci. U. S. A.* **99**:13647–13652.
23. Li Z, Chen L, Kabra N, Wang C, Fang J, Chen J. 2009. Inhibition of SUV39H1 methyltransferase activity by DBC1. *J. Biol. Chem.* **284**:10361–10366.
 24. Chini CC, Escande C, Nin V, Chini EN. 2010. HDAC3 is negatively regulated by the nuclear protein DBC1. *J. Biol. Chem.* **285**:40830–40837.
 25. Yuan J, Luo K, Liu T, Lou Z. 2012. Regulation of SIRT1 activity by genotoxic stress. *Genes Dev.* **26**:791–796.
 26. Zannini L, Buscemi G, Kim JE, Fontanella E, Delia D. 2012. DBC1 phosphorylation by ATM/ATR inhibits SIRT1 deacetylase in response to DNA damage. *J. Mol. Cell Biol.* **4**:294–303.
 27. Sapountzi V, Cote J. 2011. MYST-family histone acetyltransferases: beyond chromatin. *Cell. Mol. Life Sci.* **68**:1147–1156.
 28. Rea S, Xouri G, Akhtar A. 2007. Males absent on the first (MOF): from flies to humans. *Oncogene* **26**:5385–5394.
 29. Straub T, Becker PB. 2007. Dosage compensation: the beginning and end of generalization. *Nat. Rev. Genet.* **8**:47–57.
 30. Taipale M, Rea S, Richter K, Vilar A, Lichter P, Imhof A, Akhtar A. 2005. hMOF histone acetyltransferase is required for histone H4 lysine 16 acetylation in mammalian cells. *Mol. Cell Biol.* **25**:6798–6810.
 31. Gupta A, Guerin-Peyrou TG, Sharma GG, Park C, Agarwal M, Ganju RK, Pandita S, Choi K, Sukumar S, Pandita RK, Ludwig T, Pandita TK. 2008. The mammalian ortholog of *Drosophila* MOF that acetylates histone H4 lysine 16 is essential for embryogenesis and oncogenesis. *Mol. Cell Biol.* **28**:397–409.
 32. Thomas T, Dixon MP, Kueh AJ, Voss AK. 2008. Mof (MYST1 or KAT8) is essential for progression of embryonic development past the blastocyst stage and required for normal chromatin architecture. *Mol. Cell Biol.* **28**:5093–5105.
 33. Gupta A, Sharma GG, Young CS, Agarwal M, Smith ER, Paull TT, Lucchesi JC, Khanna KK, Ludwig T, Pandita TK. 2005. Involvement of human MOF in ATM function. *Mol. Cell Biol.* **25**:5292–5305.
 34. Sykes SM, Mellert HS, Holbert MA, Li K, Marmorstein R, Lane WS, McMahon SB. 2006. Acetylation of the p53 DNA-binding domain regulates apoptosis induction. *Mol. Cell* **24**:841–851.
 35. Tang Y, Luo J, Zhang W, Gu W. 2006. Tip60-dependent acetylation of p53 modulates the decision between cell-cycle arrest and apoptosis. *Mol. Cell* **24**:827–839.
 36. Peng L, Ling H, Yuan Z, Fang B, Bloom G, Fukasawa K, Koomen J, Chen J, Lane WS, Seto E. 2012. SIRT1 negatively regulates the activities, functions, and protein levels of hMOF and TIP60. *Mol. Cell Biol.* **32**:2823–2836.
 37. Wang C, Chen L, Hou X, Li Z, Kabra N, Ma Y, Nemoto S, Finkel T, Gu W, Cress WD, Chen J. 2006. Interactions between E2F1 and SirT1 regulate apoptotic response to DNA damage. *Nat. Cell Biol.* **8**:1025–1031.
 38. Zheng H, Chen L, Pledger WJ, Fang J, Chen J. 4 February 2013. p53 promotes repair of heterochromatin DNA by regulating JMJD2b and SUV39H1 expression. *Oncogene* [Epub ahead of print.] doi:[10.1038/onc.2013.6](https://doi.org/10.1038/onc.2013.6).
 39. Hubbard BP, Loh C, Gomes AP, Li J, Lu Q, Doyle TL, Disch JS, Armour SM, Ellis JL, Vlasuk GP, Sinclair DA. 2013. Carboxamide SIRT1 inhibitors block DBC1 binding via an acetylation-independent mechanism. *Cell Cycle* **12**:2233–2240.